Trans-epithelial migration is essential for neutrophil activation during RSV infection

Authors: Elisabeth Robinson[1], Jenny Amanda Herbert[1,2], Machaela Palor[1], Luo Ren[1,3], Isobel Larken[1], Alisha Patel[1], Dale Moulding[1], Mario Cortina-Borja[1], Rosalind Louise Smyth[1†], Claire Mary Smith[1†*].

Affiliations:
[1] UCL Great Ormond Street Institute of Child Health, London, UK.
[2] School of Medical Sciences, Faculty of Biology, Medicine & Health, University of Manchester, UK.
[3] Department of Respiratory Medicine, Children's Hospital of Chongqing Medical University, Chongqing, 400014, China

† joint senior author

* corresponding author:

Dr Claire Mary Smith,

UCL Great Ormond Street Institute of Child Health,

30 Guilford St, London WC1N 1EH, c.m.smith@ucl.ac.uk

Keywords: virus infection, bronchiolitis, airway epithelial cells, migration, movement, neutrophils

Manuscript word count - approx. 5000

Abstract

The recruitment of neutrophils to the infected airway occurs early following respiratory syncytial virus (RSV) infection and high numbers of activated neutrophils in airway and blood is associated with the development of severe disease. The aim of this study was to investigate whether trans-epithelial migration is sufficient and necessary for neutrophil activation during RSV infection.

Here, we used flow cytometry and novel live-cell fluorescent microscopy to track neutrophil movement during trans-epithelial migration and measure the expression of key activation markers in a human model of RSV infection. We found that when migration occurred, neutrophil expression of CD11b, CD62L, CD64, NE and MPO increased. However, the same increase did not occur on basolateral neutrophils when neutrophils were prevented from migrating, suggesting that activated neutrophils reverse migrate from the airway to the bloodstream side, as has been suggested by clinical observations. We then combined our findings with the temporal and spatial profiling and suggest three initial phases of neutrophil recruitment and behaviour in the airways during RSV infection; 1) initial chemotaxis; 2) neutrophil activation and reverse migration; 3) amplified chemotaxis and clustering, all of which occur within 20 minutes. This work and the novel outputs could be used to develop therapeutics and provide new insight into how neutrophil activation and a dysregulated neutrophil response to RSV mediates disease severity.

Abstract word count - 199

Introduction

Respiratory Syncytial Virus (RSV) is a seasonal respiratory virus, reported to infect almost all children before the age of 2(1). Following infection, most children develop an illness which is confined to upper respiratory tract symptoms, however 1-3% of infected infants will develop a severe illness requiring hospitalisation(2). There is no licensed vaccine for RSV and treatment is currently limited to supportive care. In resource-limited countries, RSV is a major cause of infant mortality (3–5).

Although risk factors have been identified, it is still not clear why RSV infected infants, with no apparent risk factors, require hospitalisation and respiratory support (6). One suggestion is that neutrophils, which form around 80% of all cells recovered from the airways of infants with severe RSV bronchiolitis by bronchoalveolar lavage(7), and their associated cytokines contribute to disease severity(8–10). Neutrophil mediated factors such as CXCL8 (IL-8), CXCL10 (IP-10) and neutrophil elastase are also present in substantial amounts in airway secretions of children with severe RSV bronchiolitis. (11–13).

Neutrophils are the predominant immune cell type in the systemic circulation and are the first cell recruited from the bloodstream through the airway epithelium during infection(14). Here they are thought to employ largely non-specific mechanisms of pathogen destruction including phagocytosis, neutrophil extracellular trap formation and release of toxic granule products such as neutrophil elastase and myeloperoxidase(15,16). Neutrophil trans-epithelial migration is facilitated by neutrophil receptors including integrins (i.e. CD11b) and selectins (such as CD62L) that bind to molecules on airway epithelial cells such as ICAM-1(17–19). Neutrophils also interact with other immune complexes using Fc receptors such as CD64; upregulation of CD64 has been evaluated as a biomarker for neonatal sepsis in infants(20).

Several *in vitro* and *in vivo* systems have been developed to study neutrophil migration including airway and intestinal epithelial models (21,22) We have developed an RSV infection model using primary differentiated airway epithelial cells and found that neutrophil migration resulted in increased epithelial damage and a reduced viral load (23,24). We observed that neutrophils

adhere to RSV infected AECs in a clustering pattern, which was not seen in uninfected AECs. This pattern of neutrophil chemotaxis and migration has been reported using *in vivo* models, referred to as 'neutrophil swarming' due to a resemblance with the swarming behaviour of insects (25,26). We also showed that migrated neutrophils have greater cell surface expression of CD11b and MPO compared to neutrophils that had not migrated(27). What remains unclear is whether migrated neutrophils with (i.e. higher CD11b) are selected for trans-epithelial migration or whether they become activated due to migration *per se*. Although RSV is not known to establish infection outside the respiratory tract or cause a viraemia, clinical studies have shown that a high proportion of neutrophils from the systemic circulation of infants with RSV bronchiolitis contain RSV mRNA(11). This raises the possibility that activated neutrophils, recruited to the airway during RSV infection, may be able to migrate in the reverse direction, back to the systemic circulation.

This study investigates the behaviour and function of neutrophils as they move across the airway epithelial cell layer during RSV infection. We studied this migration using a human model of primary airway epithelial cells grown at air-liquid interface for 7 days. This model facilitated the higher-resolution z-stack microscopy needed for 4D (XYZT) tracking of neutrophil migration for the first time. (**Figure 1**). We used this model to evaluate the kinetics of neutrophil trans-epithelial migration including 'cluster formation', and the temporal and spatial association of neutrophil activation during RSV infection.

Results

Neutrophil trans-epithelial migration increases damage to airway epithelial cells associated with a release of neutrophil proteases.

Firstly, as we have done before in differentiated cultures (24), we characterised whether neutrophil migration increases epithelial damage during RSV infection in our novel AEC model. As controls, we compared epithelial damage and neutrophil protease release across either 1) mock infected AECs, 2) mock infected AECs exposed to potent neutrophil chemoattractant (fMLP), or 3) mock infected AECs exposed to RSV infected AEC supernatant (referred to as RSV Sup). These controls allowed us to differentiate whether our observations were due to the process of migration *per se* or to inflammatory mediators present in the RSV infected airway supernatant.

We found that 1h after neutrophil trans-epithelial migration across epithelium infected with RSV for 24h, we detected larger gaps with mean ± standard error of the mean (SEM) of 70.8 ± 4.6% area in the RSV infected epithelial layer compared to the mock-infected (61.6 ± 6.0% area) (p<0.001) (representative images shown in **Figure 2A)**. We also detected a loss of RSV infected cells, as is observed in **Video 1**. This video shows that as neutrophil transepithelial migration progresses, a GFP-expressing AEC (i.e. positive for replicating RSV) disappears from the image, indicating loss of infected cells following neutrophil migration. A comparative video of neutrophils migrating across mock infected cells is shown in **Video 2.**

Neutrophils release several toxic products, including myeloperoxidase (MPO) and neutrophil elastase (NE). We measured the concentration of these products in the compartments of our model after neutrophil migration. We found that the concentration of NE, in airway surface media of AEC cultures, was >3 fold greater than the basolateral media following neutrophil migration across RSV infected epithelium for 4h at 72h post infection (**Figure 2B**) with a mean ± SEM of 2.0 ± 0.6mU/ml, compared to 0.6 ± 0.1mU/ml in the mock-infected cultures (p=0.039) (**Figure 2B**). We did not find a significant difference in MPO in airway surface media from RSV infected cultures following neutrophil migration for 4h compared to the mock-infected cultures.

RSV infection results in increased neutrophil adherence to AECs.

As we previously found that neutrophil adherence was associated with epithelial damage to RSV infected ciliated cultures (24), here we also counted the number of neutrophils that migrate across and adhere to AECs using fluorescence microscopy. We detected no significant difference in the concentration of key neutrophil chemoattractant IL-8 at 24h post RSV infection compared to the mock infected control (**Figure 2C)**. However, the numbers of viable neutrophils adherent to AEC cultures infected with RSV for 24h (791.1 ± 106.8 cells/cm^2) or 72h (711.1 ± 74.3 cells/cm^2) were significantly (p = 0.014) greater than the respective mock infected AEC cultures (449.8 ± 81.82 cells/cm^2) or (486.6 ± 61.5 cells/cm^2), respectively (**Figure 2D&E**). Overall, transepithelial migration did not affect neutrophil viability (**Figure 2E**). The total counts of viable neutrophils per well, i.e. combined basolateral, apically and adherent neutrophils, is shown (**Figure 2F**).

At 72h post infection, the concentration of neutrophil chemoattractant IL-8 and interferon gamma-induced protein 10 (IP-10) were significantly (p<0.05) increased in RSV infected compared to the mock infected control (**Figure 2C)**. However, we found significantly (p = 0.006) fewer neutrophils remained adherent to mock infected AECs exposed to RSV infected AEC supernatant (462.7 ± 43.3 cells/cm^2), in comparison to the RSV infected AECs (711.1 ± 74.3 cells/cm^2) (**Figure 2D**). This implies that neutrophil adherence is facilitated by RSV infected epithelial cells, rather than soluble, secreted factors released by RSV infected AECs into the supernatant. This was supported by our finding that RSV infection did not lead to an increase in the number of apical neutrophils (those that migrate and detach from the epithelial cells), with an average (mean ± SEM) of 22,876 ± 12,713 neutrophils/well, compared to the mock infected AEC cultures (19,184 ± 10,806) at 24h post infection (**Figure 2G**). Whereas significantly (p = 0.007) more apical neutrophils were recovered from mock infected AECs exposed to RSV infected AEC supernatant (RSV Sup), with an average 70,016 ± 21,115 neutrophils/well compared to the mock with 19,184 ± 10,806 and 22,876 ± 12,713 in comparison to RSV (p = 0.006) (**Figure 2G**). These data were similar at 72 hours post-infection (p = 0.980) the number of neutrophils recovered from the RSV infected AEC cultures (40,415 ± 15,143 neutrophils/well) compared to the mock (59,900 ± 18,885) (**Figure 2G**).

Neutrophils upregulate expression of key surface markers following migration across AECs

So far, this study has shown that neutrophils are capable of trans-epithelial migration across airway epithelial cells and either 'remain' on the *basolateral* side, become *adherent* to AECs, or migrate and dissociate into the *apical* space (see **Figure 1**). To determine whether the ability of a neutrophil to migrate and adhere to epithelial cells is associated with the expression of specific cellular markers associated with neutrophil activation and migration (i.e., CD11b, CD64, CD62L, NE, MPO), we analysed neutrophils recovered from basolateral, adherent, and apical compartments using flow cytometry. We chose the 72-hour timepoint following AEC infection, and 1h timepoint after neutrophil migration for these experiments as these were the conditions that resulted in the greatest number of adherent neutrophils (**Figure 2D**) to allow effective comparisons.

Firstly, as a control, we determined whether naïve neutrophils altered their expression of CD11b, CD64, CD62L, NE, MPO following exposure to epithelial-derived factors contained in

apical supernatants recovered from mock or RSV infected AECs, but in the absence of AECs (**Figure 3A**). Here, we found a significantly greater expression of CD11b on neutrophils incubated with RSV infected AEC supernatant (4,078.3 ± 109.8) compared to neutrophils incubated with media alone (1,583.7 ± 34.3) (p=0.017) or mock infected AEC supernatant (2,751 ± 37.5) (p=0.017) (**Figure 3A**). However, we found no significant difference in CD62L, CD64, NE or MPO expression on neutrophils incubated with supernatants from mock and RSV infected AECs (**Figure 3A**).

Introducing neutrophils to our migration model led to a significant increase in expression of CD11b and CD64 ($p = 0.0002$, $p = 0.005$, respectively) in neutrophils recovered from basolateral, adherent, apical compartments of RSV infected AEC models compared to neutrophils exposed to media alone (Control) (**Figure 3B**) (comparison not directly shown on graph). Interestingly, we detected a significant ($p = 0.008$) 24 and 30-fold increase ($p < 0.001$) in CD11b expression on neutrophils recovered from the *basolateral* compartments of both mock (36,708 ± 3,563) and RSV infected AECs (54,389 ± 3,863) compared to neutrophils exposed to media alone (Control) (1,583.7 ± 34.3) (**Figure 3B**).

To determine whether this was due to factors secreted into the basolateral compartment by the AECs, and therefore independent of migration, AECs were grown on membranes with a 0.4µm pore size. This smaller pore size does not permit neutrophils to move across the membrane and have contact with AECs (**Supplementary Figure S1**) but will allow for passive diffusion of secreted factors. Using this system, we found that the expression of CD11b, CD64, CD62L and MPO on basolateral neutrophils exposed to AECs grown on inserts with a 0.4µm pore size did not increase and, in fact, was no different to the values obtained in neutrophils exposed to media alone (Control). Compared to neutrophils recovered from the basolateral side of the RSV infected AEC cultures grown on 3µm inserts, neutrophils incubated on AECs grown on inserts with 0.4µm pores demonstrated CD11b, CD64, CD62L, NE and MPO levels that were at least 30x lower compared to those (**Figure 3B**). This reduction in neutrophil activation was significant ($p < 0.05$) across all groups tested (mock and RSV infected) suggesting the expression of these markers increases on neutrophils in the basolateral and adhered neutrophils because of direct contact with the AECs rather than infection (**Figure 3C**). Following trans-epithelial migration, we found that RSV infection was associated with a further 1.5-fold increase ($p = 0.021$) in CD11b expression on apical (104,145 ± 6,631) neutrophils compared to neutrophils recovered from the respective compartments of mock infected cultures (61,466 ± 4,876) (see **Figure 3B** and summarised in **Figure 3E**). There was no significant difference in CD64, CD62L, NE, MPO expression on neutrophils recovered from RSV compared to mock infected AECs (**Figure 3B**). The highest expression levels for CD11b were recorded on apical neutrophils recovered

from RSV infected AECs (104,145 ± 6,631), which was more than two-fold higher ($p < 0.05$) than both basolateral neutrophils (54,389 ± 3,863) and adherent neutrophils (53,561 ± 3,932) in the same model and >10,000-fold higher than neutrophils in media alone (Control) (1,583.7 ± 34.3) (**Figure 3B** and summarised in **Figure 3E**), suggesting that both RSV infection and migration of neutrophils was associated with this high expression of CD11b. A graphical illustration of this is shown in **Figure 3E**.

Temporal analysis of neutrophil trans-epithelial migration reveals that migrated neutrophils move slower but farther during RSV infection

We used time-lapse fluorescence microscopy imaging and performed vector analysis (or XYZ coordinates) of fluorescently labelled neutrophils to determine differences in the speed, track duration, distance travelled and directionality of neutrophils (n=200 per condition) during trans-epithelial migration through mock and RSV infected AECs.

SPEED We found that, over the course of the first hour, neutrophils' average (mean ±SEM) speed across RSV infected AECs was significantly ($p<0.001$) slower (2.28μm/sec ± 0.008) than the average speed of neutrophils moving through the mock infected AECs (4.18μm/sec ± 0.14) (**Figure 4A)**. The exception to this was the first 15 minutes of exposure, where we found no significant difference in speed of neutrophils migrating across RSV and mock infected AECs (**Figure 4A)**.

To determine whether this was associated with chemoattractants in the apical supernatant, we tracked the movement of naive neutrophils towards apical supernatants collected from RSV or mock infected AEC cultures using specialised 2D chemotaxis chambers (**Figure 4B**). Here, we found that neutrophils exposed to supernatants collected from RSV infected AEC cultures moved faster (0.205 μm/sec ± 0.001) than neutrophils exposed to supernatant collected mock treated AECs (0.110μm/sec ± 0.001) ($p < 0.05$) (**Figure 4B**). At their fastest recorded speed (0.568μm/sec ± 0.049), neutrophils exposed to supernatants collected from RSV infected AECs were 1.5 times faster ($p = 0.018$) than those migrating toward supernatant collected from mock treated AECs (0.377μm/sec ± 0.014). There was no significant difference between the neutrophils exposed to media only.

DURATION Measuring cumulative displacement (i.e., total distance travelled), we found that neutrophils exposed to supernatants collected from RSV infected AECs moved significantly ($p= 0.016$) further (349μm ± 49.9) than those exposed to media alone (182.7μm ± 8.96) (**Figure 4C**). We also measured the duration of neutrophil tracks during trans-epithelial migration (i.e.,

the length of time each neutrophil interacts with epithelium). Here we found that neutrophils interacted with RSV infected AECs (368μm ± 49.9) for longer than mock infected AECS (**Figure 4D**). We found no significant difference in linearity, or 'track straightness' between neutrophils observed migrating through RSV infected AECs or the mock (**Supplementary Figure S2).** However, neutrophils moving through mock infected AECs showed significantly (p<0.001) greater total displacement (137.19μm ± 4.51) compared to those moving through RSV infected AECs (107.05μm ± 4.86) (**Figure 4E**).

DIRECTIONALITY We performed some preliminary analysis of the Z-tracks of neutrophils (n=20) migrating across RSV infected AECs (3 representative tracks **Supplementary Figure S3**). This showed preliminary evidence that neutrophils may move bidirectionally across the AECs, migrating to the apical side of RSV infected airway epithelium and returning to the basolateral compartment, as soon as 15 minutes after migration. This supports the hypothesis that the increased CD11b expression in neutrophils in the basolateral compartment is due to a proportion of those neutrophils having undergone reverse migration.

Neutrophil clustering occurs 20 minutes after neutrophil recruitment

We previously observed that neutrophils adherent to RSV infected epithelium formed large clusters (24). Here, we aimed to quantify this clustering and determine whether it was significantly enhanced during RSV infection. To do this we first determined the expected nearest neighbour median distance, assuming an even distribution of the average number of adherent neutrophils. As more neutrophils are adherent to RSV infected AECs compared to mock infected, we determined that the median distance of the *expected* nearest neighbour was shorter in RSV infected AEC cultures (140μm ± 24.3) in comparison to neutrophils adherent to the mock infected epithelium (169.4μm ± 57.8). The *observed* nearest neighbour median distance was also shorter in RSV infected AEC cultures (61.32μm ± 30.9) in comparison to neutrophils adherent to the mock infected epithelium (119.4μm ±51.6) (**Figure 5B**). Importantly, the observed distances between neutrophils adherent to RSV infected AECs (61.32μm ± 30.9) was significantly (p<0.001) shorter than the expected distance (140μm ± 24.3) (**Figure 5B**). This indicates that the distribution of these adherent neutrophils on the epithelial surface is neither random nor uniform.

We then determined when, during trans-epithelial migration, neutrophils begin to cluster to RSV infected AECs. This was defined as the earliest timepoint that the observed and expected nearest neighbour median distance became significantly different (**Figure 5C**). We found that

after 20 minutes, the observed median (± interquartile range (IQR)) difference between neutrophils and their nearest neighbours (102.9μm ± 55.8) was significantly shorter ($p < 0.001$) than the distance expected by chance alone (140μm ± 24.3) (**Figure 5C)**. This suggests that neutrophil clustering begins to occur around 10 mins after the addition of neutrophils to the basolateral side of AECs in our model. Between 10-20 minutes we detected a more marked rate of decline in nearest neighbour distance to 42.9μm ±55.8. After this time phase, and between 20-60 minutes, the mean distance to nearest neutrophil stays constant around 50μm (**Figure 5C).**

Location of neutrophil clustering is initiated by a dying neutrophil.

In order to observe the initiation of neutrophil clustering to RSV infected AECs we used a higher-speed and resolution image capture system (see **Video 3)**. Here neutrophils, labelled with a fluorescent viability stain (calcein red-orange), were found to rapidly nucleate and form a cluster on the apical side of the AECs approx. 20 minutes after the basolateral addition of neutrophils (**Figure 5DEF**). This pattern of clustering bears resemblance to previous *in vivo* work which described this observation as neutrophil swarming (26). Previous in vitro assays with bacteria have indicated that dying neutrophils precede the swarm-like formation of neutrophil clusters(28). To determine probable source of the nucleation point in our model, we segmented a region of interest immediately adjacent to the cluster nucleus (shown in **Figure 5D**) and tracked the neutrophils in the preceding 0-20 minutes. This data (**Figure 5GH**) shows that the timing of the death (loss of viability stain) of a single neutrophil (labelled #1 in Figure 5GH) correlated to the amplified recruitment of the neutrophil population at 20 min, that was directed towards the unviable neutrophil (see **Video 4)**. This indicates that neutrophil death may serve as a catalyst for swarming during RSV infection.

Discussion

This study has, for the first time, performed spatial, temporal and functional analysis on migrating neutrophils in response to RSV infection of primary human airway epithelial cells. Our findings identify three putative phases of neutrophil migration:

1) Initial chemotaxis and adherence
2) Activation and reverse migration

3) Amplified chemotaxis and clustering

Firstly, we found that RSV infection led to greater, but slower, net movement of neutrophils across RSV infected AECs in comparison to mock infected AECs. This contradicted with our findings that, in the absence of AECs, neutrophils moved faster towards RSV infected supernatants (that contained elevated levels of the potent neutrophil chemoattractants CXCL8 (IL-8) and CXCL10 (IP-10) (**Supplementary Figure S2**), compared to neutrophils exposed to mock infected AEC supernatants. This suggests that an airway epithelial cell factor is responsible for slowing down the migration of neutrophils in the RSV infected AEC model. This could be due to the interaction of epithelial ICAM-1 to neutrophil integrin LFA-1, as we have previously shown (30). Alternatively, cell syncytia formation, a known histopathological characteristic of RSV infection, could increase epithelial impedance by reducing the availability of accessible cell-cell junctions through which migration may occur(30,31). This may not only slow down the initial neutrophil response to RSV infection, but also prolong its duration and slow its resolution, contributing to a heightened period of inflammation.

Secondly, we found that trans-epithelial migration led to apical (but not basolateral) secretion of soluble neutrophil granular factors including MMP9, myeloperoxidase (MPO), and neutrophil elastase (NE) that correlated to epithelial damage. Migration also led to greater expression of neutrophil activation markers CD11b, CD64, CD62L, NE and MPO, with highest expression recorded on neutrophils recovered from the apical compartment of RSV infected AECs. Interestingly, neutrophils recovered from *basolateral* compartments of the AEC model also increased expression of CD11b, CD64, CD62L and MPO, but not NE, compared to the media and epithelial-derived supernatant controls. This is supported by clinical studies of children hospitalised with RSV bronchiolitis, which showed that neutrophils with upregulated CD11b were recoverable both from the airways by bronchiolar lavage and from peripheral circulation(9). Furthermore, neutrophils recovered from peripheral circulation of infants with RSV bronchiolitis have been shown to contain RSV mRNA(11). Viraemia due to RSV has not, to our knowledge, been observed clinically, which suggests that the virus causes symptoms because of its effects on the respiratory tract. This poses an important question: are activated neutrophils preferentially selected for migration or does the process of trans-epithelial migration increase expression of neutrophils activation markers? To address this, we cultured our AECs on membrane inserts with a smaller pore size (0.4µm), that prevented neutrophil migration. Here, following RSV infection, we did not find any difference in CD11b, CD64, CD62L and MPO

expression on basolateral neutrophils compared to neutrophils exposed to media alone. This suggests that neutrophils increase their expression of CD11b, CD64, CD62L and MPO during or following migration, rather than an existing sub-population of activated neutrophils being selected for migration. This was different for NE. Here we detected a decrease in NE expression when neutrophils were exposed to basolateral side of RSV infected AECs, compared to mock infected. as a similar pattern in NE expression is seen when comparing neutrophils exposed to the no-AEC mock and RSV supernatants, suggesting that secreted factors may drive this change. Therefore, the presence of these 'activated' neutrophils on the *basolateral* side of the AECs following migration, may suggest that neutrophils, which are 'activated' by the apical environment, reverse migrate to the basolateral side of AECs (see Graphical Abstract). To investigate this further, we analysed the Z-tracks of neutrophils migrating across RSV infected AECs (**Supplementary Figure S3**). This showed that neutrophils can move bidirectionally across the AECs, quickly migrating to the apical side of RSV infected airway epithelium and returning to the basolateral compartment, as soon as 15 minutes after migration. This important finding may suggest that reverse migrating neutrophils have the ability to re-enter the peripheral circulation and contribute to vascular leakage or parenchymal necrosis, as seen in severe cases of RSV bronchiolitis(32).

Next, we found that RSV infection led to greater numbers of neutrophils remaining adherent to RSV infected AECs. This may be due to increased expression of host cell receptors including ICAM-1 (intercellular adhesion molecule 1), which we (and others) have previously shown to be upregulated *in vitro* airway models of RSV infection, and mediate neutrophil adherence to RSV infected AECs (24,30) (30) In support of this, we found that fewer neutrophils remained adherent to mock infected AECs exposed to RSV infected supernatant placed apically (in comparison to RSV infected AECs). This suggests that properties of the epithelial cells, rather than the apical milieu of the RSV infected epithelium *per se*, are responsible for neutrophil adherence. Interestingly, neutrophils were observed to adhere in clusters to the apical surface of RSV infected AECs. Neutrophil clustering has been shown as a vital mechanism for host defence against pathogens(22,24). However, large clusters have been associated with inflammatory disease in both human and murine models(33,34). In models of RSV infection, increased neutrophil adherence and clustering has been associated with greater AEC damage (23,24,35,36).

To examine the formation of these clusters in more detail, we used higher-resolution time-lapse microscopy to image the early movement of neutrophils moving across RSV infected AECs. This showed that clusters can result from the coordinated convergence of neutrophils, which resembled reports of neutrophil swarming in response to infection and sterile injury in *in vivo* models (24–26). This pattern of neutrophil movement is thought to be initiated by the release of danger-associated molecular patterns (DAMPs) from neutrophils, which induce a transcriptional switch in their neighbours and coordinate a collective movement (37). LTB4 is a leukotriene DAMP, released by dying neutrophils and has been shown to mediate this directed leukocyte movement previously (26,33,38,39). We also showed that neutrophil death, or loss of cell viability, may serve as a catalyst for swarming during RSV infection. Here, we speculate that the formation of clusters of neutrophils, seen in our model, is not mediated by the RSV infected AECs, but instead due to neutrophils themselves triggering and maintaining clustering behaviour. The ability of neutrophils to affect others around them is an emerging area of research, and neutrophil quorum signalling has been shown to coordinate neutrophil collective responses to wound healing(25,26,40). Whether this response is a natural protective mechanism in countering an RSV infection or an aberrant response remains to be fully explained, but focal damage to AECs *in vivo* may allow increased neutrophil migration.

In summary, neutrophil activation has been shown as a key precursor to the development of severe respiratory symptoms in children with RSV bronchiolitis (41). Here we have shown that contact of neutrophils with AECs and/or trans-epithelial migration through RSV infected AECs is essential for upregulation of neutrophil activation markers, including CD11b expression. We describe distinct, measurable patterns of neutrophil movement, including the formation of neutrophil clusters on RSV infected AECs. We present evidence of the bidirectional movement of neutrophils across AECs during RSV infection and return of activated neutrophils to the basolateral side of infected AECs. This could explain how neutrophils with upregulated CD11b and presence of viral products were recoverable in blood neutrophils of babies with RSV bronchiolitis (9,11,25,37,40) and could have important systemic implications for severe disease sequalae. This is a critical area for discovery and the model that we have developed here could be used to unravel important disease mechanisms, including the key question of how RSV accesses extra-pulmonary sites during infection. Future work should include the identification of new biomarkers of specific neutrophils sub-populations responsible for driving severe disease

outcomes; screening anti-inflammatory drugs; and determining new mechanisms that may aid disease resolution.

Materials and Methods

Participants

Peripheral blood and airway epithelial cells were obtained from healthy adult donors at UCL GOS Institute of Child Health. Written informed consent was obtained from all donors prior to their enrolment in the study. Study approval was obtained from the UCL Research Ethics Committee (4735/002). All methods were performed in accordance with the relevant guidelines and regulations.

Neutrophil Isolation

Venous blood was collected in EDTA (Ethylene Diamine Tetra Acetic) tubes (Greiner). Neutrophils were then ultra-purified using an EasySep Direct Neutrophil isolation kit (Stem Cell Technologies) according to the manufacturer's instructions and subsequently stained with Cell Trace Calcein Red-Orange cell stain (ThermoFisher) and processed as described previously (27).

Transepithelial Migration Model

This study modified the transepithelial migration model described by Herbert et al (2020) to utilise undifferentiated human AECs, grown at air liquid interface for 7 days as opposed to 28-day ciliated cultures. This ensures a flatter more uniform culture which is possible to live image using confocal microscopy(24). AECs cells were cultured on porous PET inserts (Greiner) with pore size of 3μm to allow migration or 0.4μm to prohibit it. AEC cultures were infected with RSV 24 or 72 hours prior to the addition of neutrophils. Mock infected AECs with RSV infected AEC supernatant were used as a control (RSV Sup), as were mock infected AECs with n-Formylmethionine-leucyl-phenylalanine (fMLP) 100nM placed apically as a positive control for neutrophil chemotaxis. 400μl of supernatant was added underneath the membrane insert for each experimental group, Mock, RSV, RSV supernatants only and fMLP control. Excess supernatant prior to neutrophil migration was stored at -20^{o}C for use in chemotaxis and activation experiments. Neutrophils were then added to the basolateral side of all membrane

inserts, then left to incubate for 1 or 4 hours. After migration, neutrophils were collected from the apical side of the epithelial cells for quantification. Supernatants were collected and membrane inserts were fixed and stained. Mock infection was performed by inoculating with sterile media in the place of viral inoculum.

Virus purification and quantification

Recombinant GFP tagged RSV A2 strain was kindly provided by Jean-Francois Eleouet and described in Fix et al(42). Viral stock preparation and quantification of viral titre was performed using HEp-2 cells (ATCC CCL-23) was performed as described previously(24).

Microscopy

AEC cultures were fixed for microscopy using 4% paraformaldehyde (v/v) and mounted using 0.1M n-Propyll Gallate in glycerol:PBS (9:1). Images of fixed cultures were acquired using an inverted Zeiss LSM 710 confocal microscope using a 20x Plan Achromat LWD objective. Live cell imaging was performed using a Perkin Elmer UltraView spinning disk (CSU22) confocal microscope. All microscopes were located in the UCL GOS Institute of Child Health Imaging Facility (London, UK).

Quantification of migrated and adherent neutrophils

The number of migrated neutrophils was quantified as described previously (24). Flow cytometric analysis of CD11b, NE, MPO, CD64 and CD62L expression was performed as described previously(23). Antibodies used are provided in supplementary information. Image acquisition was the same as above. Neutrophils were counted using an ImageJ counting tool.

Quantifying neutrophil distribution

To investigate whether neutrophil adherence to AECs was uniform (null hypothesis =0) or whether they clustered, a method of measuring neutrophil distribution was required. Images taken of AECs after 1 hour of migration were taken as described previously, then analysed using ImageJ to first identify neutrophils within the image, determine their 3D coordinates. These coordinates were then exported into R and analysed using the R package `spatstat` to then calculate the distance between the centre-point of each neutrophil and the centre-point of its five nearest neighbours (43). However, it is expected that if more neutrophils are adherent to RSV infected AECs in comparison to mock, that they would be closer together by crowding

alone. To account for this, the distance apart each neutrophil would be if neutrophils were evenly spread over the AEC area was calculated from the numbers of neutrophils counted as adherent to the same AECs. ImageJ macro code for determining 3D coordinates and subsequent R code for distance analysis is available upon request.

Analysis of neutrophil chemotaxis

Time-lapse videos were analysed using Icy (https://icy.bioimageanalysis.org/) , programmed to run a spot detection protocol for each frame of the stack, detecting light objects close to 10µm diameter on a dark background to identify neutrophils within the image. Then, a spot tracking plugin was used to map the displacement of each neutrophil through each time point image (44). The tracks produced were then visually checked for tracking accuracy and where erroneous tracks were found, corrected manually, or removed from analysis. Raw spot files and track files were exported for further analysis using R. Data sets detailing total displacement, net displacement, average, maximum and minimum speed, and linearity were exported combined with replicate data sets for analysis using R and GraphPad Prism v8.0.

Time-lapse imaging of neutrophil trans-epithelial migration in 4D (XYZT)

A black plastic 24 well plate with a glass coverslip bottom (Greiner) was used in place of a low binding 24 well plate (Greiner) to allow for live imaging of AEC cultures during trans-epithelial migration. Neutrophils were identified using Icy and a spot detection protocol initiated for each frame of the stack, detecting light objects close to 10µm diameter on a dark background. Then each spot was tracked using the spot tracking plugin using a 4D tracking algorithm (44). Tracks were then visually checked for tracking accuracy and where erroneous tracks were found, were either corrected manually or removed from analysis. Raw track coordinates were exported for further analysis using R package `motilitylab` (45). Data detailing displacement, speed and linearity were exported. Analysis of neutrophil movement and distribution was performed using the R packages `motilitylab`, `spatstat` and `dpylr` (46–48).

Acknowledgements

LR was recipient of a Newton fellowship from The Academy of Medical Science (ref NIF004/1012). RLS was supported by the Great Ormond Street Children's Charity (grant code W1802). CMS is a recipient of grants from Animal Free Research UK (AFR19-20274), BBSRC (BB/V006738/1), GOSH Children's charity (COVID_CSmith_017) and the Wellcome Trust

(212516/Z/18/Z). This research was supported by the NIHR Great Ormond Street Hospital Biomedical Research Centre. Microscopy was performed at the Light Microscopy Core Facility, UCL GOS Institute of Child Health supported by the NIHR GOSH BRC award 17DD08.The views expressed are those of the author(s) and not necessarily those of the NHS, the NIHR or the Department of Health. We thank Dr Shyam Sawhney for technical support and the healthy volunteers who donated airway cells and blood samples for this study

Author contributions

All authors declare no conflicts of interest.

ER conceived and designed the study, conducted experiments, analysed data, and prepared the manuscript. JAH designed the study, conducted experiments, analysed data, and reviewed the manuscript. MP assisted with flow cytometry data analysis and review of the manuscript. LR, IL, and AP assisted with data collection and review of the manuscript. DM assisted with microscopy acquisition and reviewed the manuscript. MC-B conducted statistical analysis and reviewed the manuscript. RLS and CMS oversaw the funding application and contributed to study conception and design, data analysis and interpretation, and the write-up of the manuscript.

References

1. Glezen WP, Taber LH, Frank AL, Kasel JA. Risk of primary infection and reinfection with respiratory syncytial virus. Am J Dis Child. 1986 Jun;140(6):543–6.
2. Hall CB, Weinberg GA, Iwane MK, Blumkin AK, Edwards KM, Staat MA, et al. The Burden of Respiratory Syncytial Virus Infection in Young Children. New England Journal of Medicine. 2009 Feb 5;360(6):588–98.
3. Smyth RL, Openshaw PJ. Bronchiolitis. Vol. 368, Lancet. 2006. p. 312–22.
4. Shi T, McAllister DA, O'Brien KL, Simoes EAF, Madhi SA, Gessner BD, et al. Global, regional, and national disease burden estimates of acute lower respiratory infections due to respiratory syncytial virus in young children in 2015: a systematic review and modelling study. The Lancet. 2017 Sep 2;390(10098):946–58.
5. Nair H, Nokes DJ, Gessner BD, Dherani M, Madhi SA, Singleton RJ, et al. Global burden of acute lower respiratory infections due to respiratory syncytial virus in young children: a systematic review and meta-analysis. The Lancet. 2010;375(9725):1545–55.
6. Geoghegan S, Erviti A, Caballero MT, Vallone F, Zanone SM, Losada JV, et al. Mortality due to respiratory syncytial virus. burden and risk factors. Am J Respir Crit Care Med. 2017 Jan;195(1):96–103.
7. McNamara PS, Ritson P, Selby A, Hart CA, Smyth RL. Bronchoalveolar lavage cellularity in infants with severe respiratory syncytial virus bronchiolitis. Arch Dis Child. 2003 Oct 1;88(10):922–6.
8. Openshaw PJ, Chiu C. Protective and dysregulated T cell immunity in RSV infection. Vol. 3, Current Opinion in Virology. Elsevier B.V.; 2013. p. 468–74.
9. Halfhide CP, Brearey SP, Flanagan BF, Hunt JA, Howarth D, Cummerson J, et al. Neutrophil TLR4 expression is reduced in the airways of infants with severe bronchiolitis. Thorax [Internet]. 2009 Sep 1 [cited 2018 Aug 16];64(9):798–805. Available from: http://dx.doi.org/10.1136/thx.2008.107821
10. Openshaw PJMM, Chiu C, Culley FJ, Johansson C. Protective and Harmful Immunity to RSV infection. Annu Rev Immunol. 2017 Apr 26;35(1):501–32.
11. Halfhide CP, Flanagan BF, Brearey SP, Hunt JA, Fonceca AM, McNamara PS, et al. Respiratory syncytial virus binds and undergoes transcription in neutrophils from the blood and airways of infants with severe bronchiolitis. J Infect Dis [Internet]. 2011 Aug;204(3):451–8. Available from: http://dx.doi.org/10.1093/infdis/jir280
12. Smyth RL, Mobbs KJ, O'Hea U, Ashby D, Hart CA. Respiratory syncytial virus bronchiolitis: Disease severity, interleukin-8, and virus genotype. Pediatr Pulmonol. 2002 May 1;33(5):339–46.
13. Bataki EL, Evans GS, Everard ML. Respiratory syncytial virus and neutrophil activation. Clin Exp Immunol. 2005 Jun;140(3):470–7.
14. Erhlich P, Lazarus E. Die Anaemie. Wein. 1898;8(49).
15. Papayannopoulos V. Neutrophil extracellular traps in immunity and disease. Nat Rev Immunol. 2018 Feb 1;18(2):134–48.
16. Cannon MJ, Openshaw PJM, Askonas BA. Cytotoxic T cells clear virus but augment lung pathology in mice infected with respiratory syncytial virus. Journal of Experimental Medicine. 1988 Sep 1;168(3):1163–8.
17. Chin AC, Parkos CA. Pathobiology of neutrophil transepithelial migration: implications in mediating epithelial injury. Annu Rev Pathol. 2007;2:111–43.

1. Lyck R, Enzmann G. The physiological roles of ICAM-1 and ICAM-2 in neutrophil migration into tissues. Curr Opin Hematol. 2015 Jan;22(1):53–9.
2. REBUCK N, GIBSON A, FINN A. Neutrophil adhesion molecules in term and premature infants: normal or enhanced leucocyte integrins but defective L-selectin expression and shedding. Clin Exp Immunol. 2008 Jun 28;101(1):183–9.
3. Elawady S, Botros SK, Sorour AE, Ghany EA, Elbatran G, Ali R. Neutrophil CD64 as a diagnostic marker of sepsis in neonates. Journal of Investigative Medicine. 2014;62(3):644–9.
4. Sumagin R, Robin AZ, Nusrat A, Parkos CA. Transmigrated neutrophils in the intestinal lumen engage ICAM-1 to regulate the epithelial barrier and neutrophil recruitment. Mucosal Immunology 2014 7:4 [Internet]. 2013 Dec 18 [cited 2022 Nov 24];7(4):905–15. Available from: https://www.nature.com/articles/mi2013106
5. Yonker LM, Mou H, Chu KK, Pazos MA, Leung H, Cui D, et al. Development of a Primary Human Co-Culture Model of Inflamed Airway Mucosa. Sci Rep [Internet]. 2017 Aug;7(1):8182. Available from: http://dx.doi.org/10.1038/s41598-017-08567-w
6. Deng Y, Herbert JA, Robinson E, Ren L, Smyth RL, Smith CM. Neutrophil: Airway Epithelial Interactions Result in Increased Epithelial Damage and Viral Clearance during RSV Infection. J Virol. 2020 Apr 15;
7. Herbert JA, Deng Y, Hardelid P, Robinson E, Ren L, Moulding D, et al. β2 integrin LFA1 mediates airway damage following neutrophil trans-epithelial migration during RSV infection. European Respiratory Journal. 2020 Mar 26;1902216.
8. Poplimont H, Georgantzoglou A, Boulch M, Walker HA, Coombs C, Papaleonidopoulou F, et al. Neutrophil Swarming in Damaged Tissue Is Orchestrated by Connexins and Cooperative Calcium Alarm Signals. Current Biology. 2020;
9. Lämmermann T, Afonso P V., Angermann BR, Wang JM, Kastenmüller W, Parent CA, et al. Neutrophil swarms require LTB4 and integrins at sites of cell death in vivo. Nature. 2013 Jun 26;498(7454):371–5.
10. Deng Y, Herbert JA, Smith CM, Smyth RL. An in vitro transepithelial migration assay to evaluate the role of neutrophils in Respiratory Syncytial Virus (RSV) induced epithelial damage. Sci Rep [Internet]. 2018 Dec 30 [cited 2018 Sep 5];8(1):6777. Available from: http://www.nature.com/articles/s41598-018-25167-4
11. Guggenberger C, Wolz C, Morrissey JA, Heesemann J. Two Distinct Coagulase-Dependent Barriers Protect Staphylococcus aureus from Neutrophils in a Three Dimensional in vitro Infection Model. PLoS Pathog [Internet]. 2012 Jan [cited 2022 Jun 30];8(1):e1002434. Available from: https://journals.plos.org/plospathogens/article?id=10.1371/journal.ppat.1002434
12. R Core Team (2021). R: A language and environment for statistical computing. . R Foundation for Statistical Computing, Vienna, Austria.;
13. Wang SZ, Hallsworth PG, Dowling KD, Alpers JH, Bowden JJ, Forsyth KD. Adhesion molecule expression on epithelial cells infected with respiratory syncytial virus. European Respiratory Journal. 2000 Feb 1;15(2):358–66.
14. Tian J, Huang K, Krishnan S, Svabek C, Rowe DC, Brewah Y, et al. RAGE inhibits human respiratory syncytial virus syncytium formation by interfering with F-protein function. J Gen Virol. 2013 Aug;94(Pt 8):1691–700.
15. Smyth RL, Brearey SP. BRONCHIOLITIS. Encyclopedia of Respiratory Medicine [Internet]. 2006 Jan 1 [cited 2022 Nov 24];268. Available from: /pmc/articles/PMC7149666/

31. Song Z, Huang G, Paracatu LC, Grimes D, Gu J, Luke CJ, et al. NADPH oxidase controls pulmonary neutrophil infiltration in the response to fungal cell walls by limiting LTB4. Blood. 2020 Mar 19;135(12):891–903.
34. Alex H, Scherer A, Kreuzburg S, Abers MS, Zerbe CS, Dinauer MC, et al. Neutrophil swarming delays the growth of clusters of pathogenic fungi. Nat Commun. 2020 Dec 1;11(1).
35. Grommes J, Soehnlein O. Contribution of neutrophils to acute lung injury. Mol Med. 2011;17(3–4):293–307.
36. Wang SZ, Xu H, Wraith A, Bowden JJ, Alpers JH, Forsyth KD. Neutrophils induce damage to respiratory epithelial cells infected with respiratory syncytial virus. Eur Respir J. 1998 Sep 1;12(3):612–8.
37. Vanhook AM. Coordinating a neutrophil swarm. Vol. 13, Science Signaling. American Association for the Advancement of Science; 2020.
38. Subramanian BC, Majumdar R, Parent CA. The role of the LTB4-BLT1 axis in chemotactic gradient sensing and directed leukocyte migration. Vol. 33, Seminars in Immunology. Academic Press; 2017. p. 16–29.
39. Wan M, Tang X, Stsiapanava A, Haeggström JZ. Biosynthesis of leukotriene B4. Vol. 33, Seminars in Immunology. Academic Press; 2017. p. 3–15.
40. Palomino-Segura M, Hidalgo A. Immunity: Neutrophil quorum at the wound. Curr Biol. 30:R828–30.
41. MS H, RS T, M C, A J, A P, F K, et al. Neutrophilic inflammation in the respiratory mucosa predisposes to RSV infection. Science [Internet]. 2020 Oct 9 [cited 2021 Sep 15];370(6513). Available from: https://pubmed.ncbi.nlm.nih.gov/33033192/
42. Fix J. The Insertion of Fluorescent Proteins in a Variable Region of Respiratory Syncytial Virus L Polymerase Results in Fluorescent and Functional Enzymes But with Reduced Activities. Open Virol J. 2011 Sep 6;5(1):103–8.
43. Bolte S, Cordelières FP. A guided tour into subcellular colocalization analysis in light microscopy. Vol. 224, Journal of Microscopy. Blackwell Publishing Ltd; 2006. p. 213–32.
44. Chenouard N, Bloch I, Olivo-Marin JC. Multiple hypothesis tracking for cluttered biological image sequences. IEEE Trans Pattern Anal Mach Intell. 2013;35(11):2736–50.
45. Dannenberg K, Berry J, Maintainer JT, Textor J. Package "MotilityLab" Type Package Title Quantitative Analysis of Motion. 2016 [cited 2020 Aug 5]; Available from: http://www.motilitylab.net
46. Textor J; Dannenberg K; Berry J; Burger G (2016) R Package motiltylab, version 0.25. http://www.motilitylab.net.
47. Baddeley A; Turner R (2005). spatstat: An R Package for Analyzing Spatial Point Patterns. Journal of Statistical Software 12(6), 1-42. URL http://www.jstatsoft.org/v12/i06/.
48. Wickham, H; François R; Henry L; Müller K (2021). dplyr: A Grammar of Data Manipulation. R package version 1.0.7. https://CRAN.R-project.org/package=dplyr.

Figure Legends

Figure 1 – Schematic of method and model used to study neutrophil trans-epithelial migration in response to RSV infection. Human primary airway epithelial cells (AECs) were cultured on the underside of a 3μm pore size, transparent PET culture membrane insert. AECs were matured at an air-liquid interface (ALI) for 7 days before infection with GFP tagged RSV. At this time, neutrophils, stained with a viability stain (calcein-red orange), were added to the basolateral side of AEC cultures and a 50μm Z-stack image of the focal area indicated was captured for up to 1hr. Drawing created using Biorender.com

Figure 2 RSV increases the numbers of neutrophils that adhere to RSV infected epithelial cultures, forming clusters on the AEC surface. (A) – Representative image showing neutrophil (red cells) adherence to epithelial cells (DAPI staining – blue) following migration for 1h at 24h or 72h post RSV or mock infection. fMLP 1ng/ml placed apical to uninfected AECs was used a positive control for neutrophil chemotaxis. Scale bar indicates 50μm (B) – Soluble granular factors myeloperoxidase (MPO), neutrophil elastase (NE) and matrix-metalloproteinase-9 (MMP-9) in the apical supernatant (designated AS in figure) and basolateral supernatant (BS) were quantified using ELISA. fMLP and mock infected AECs with supernatant collected from RSV infected AECs placed apically (RSV Sup). (C) Concentration of IL-8 and IP-10 in the apical supernatants from RSV infected AECs (green) or Mock (blue) infected AECs infected for 24 or 72 hours. Groups were compared with One-Way ANOVA with Tukey's post hoc adjustment for multiple testing. *= $p<0.05$. **=$p<0.002$. (D) Graph showing representative counts of neutrophils isolated either basolateral to, apical to or adherent to AECs. Absolute counts performed using a flow cytometer selecting for neutrophils as positive for CD11b-APC antibody staining. (E) – Representative 2 channel maximum intensity projection of a Z-stack image (50μm range) of 72-hour mock (top) and RSV (bottom) showing neutrophil adherence in clusters to mock and RSV infected AECs. Green = gfpRSV infected AECs, red=neutrophils. Scale bar indicates 100μm (F)– Numbers of neutrophils adherent to AECs after 1hr transepithelial migration across 24 or 72 hr RSV infected AECs. Adherent neutrophils and epithelial cells were counted using ImageJ counting tool, the average number of neutrophils from all images is shown. (G)- Numbers of neutrophils migrating and dissociating apically from AECs after 1hr transepithelial migration across 24 or 72 hr RSV infected AECs. Neutrophil concentrations were quantified in the apical surface media using a plate reader and read against a standard curve.

Figure 3 Neutrophils undergoing trans-epithelial migration alter their expression of surface markers depending on their location. (A) Mean fluorescence intensity (MFI) of cell surface expressed CD11b, CD64, CD62L, NE, MPO on neutrophils incubated for 1h with media alone (Control) or media containing supernatant recovered from RSV or mock infected AECs. No airway epithelial cells were present in this model. Only a significant increase in CD11b was detected in this model between neutrophils exposed to RSV compared to mock infected supernatant. (B) MFI of the same neutrophil markers as A) but these were measured on neutrophils recovered after 1h exposure to our airway epithelial migration model. Data show the MFI of markers on neutrophils recovered from the basolateral, adherent, and apical (migrated) compartments within the assay migration across mock or RSV infected AEC cultures. AECs were grown on membrane inserts with a 3μm or 0.4μm pore size, the latter prevents cellular migration (see Supplementary Figure S1). P values show significant difference between 0.4um model for RSV infection condition. Red # represents a significant ($p<0.05$) difference between mock and RSV conditions for that neutrophil population using wilcox-signed rank test n=4. C) Correlation of CD11b expression with other markers measured showing clustering of migrated neutrophils in top right section of graph. (D) Heatmap summary of MFI of neutrophils exposed to supernatant alone or the migration model. A linear of mixed effects model was fitted to compare interactions between infection and location groups accounting for intra-donor variability. Individual comparisons performed with Two-Way ANOVA with pairing and Tukey's post hock test. * = in comparison to respective basolateral group # = in comparison to respective adherent group. (E) Graphical illustration of possible interpretation of findings of CD11b expression Left panel shows primary airway epithelial cells cultured at ALI on membrane inserts with 3μm pore size that permits neutrophils to migrate through. 1) unmigrated neutrophils expressing baseline levels of CD11b, 2) neutrophils migrate across infected AECs and some remain adherent to the infected AECs, 3) neutrophils are shown to increase expression of CD11b and other activation associated markers, 4) some 'activated' neutrophils undergo reverse migration as 5) neutrophils with the increased expression of CD11b are detected on the basolateral side of the insert. Right panel shows primary airway epithelial cells cultured at ALI on membrane inserts with 0.4μm pore size that prevents neutrophil contact with AECs and migration. Here, after 1h incubation with RSV infected AECs, neutrophils on the basolateral side 1) and 2) were shown to express the same level of CD11b markers, indicating that neutrophil contact with AECs and starting to move through the AECs is key process for increasing expression of these activation markers. Drawing created using BioRender.com

Figure 4 Neutrophil trafficking and directionality when exposed to supernatants from or RSV infected AECs (green) or Mock (blue) infected AECs infected for 72 hours. A) Average neutrophil speed during trans-epithelial migration across mock and RSV infected AECs. This time series was split into 15-minute segments. B) 2D Chemotaxis in ibidi chemotaxis chambers showing the average speed neutrophils move in response to apical supernatants from AECs. C) Neutrophil displacement – the gross distance travelled by individual neutrophils in response to apical supernatants from AECs. D) Average track duration of 200 individual neutrophils during movement through mock and RSV infected AECs. Speed of tracks were calculated using motilityLab. E) Mean squared displacement of neutrophils at each time point during movement across mock and RSV infected AECS. Statistical analysis between groups were performed using a Wilcoxon-Mann- Whitney U test, where significance was found this is indicated on the chart. *** $p < 0.001$. F) Visualisation of 50 tracks

Figure 5A– Distribution analysis of neutrophils adherent to AECS infected with mock (left panel) and RSV (right panel) for 72h following trans-epithelial migration. AECs were fixed after 1 hour; neutrophil position was processed using ImageJ and coordinates analysed using R version 4.0.3. B) Histogram showing the frequency of neutrophils the distribution of distance to nearest neighbouring neutrophil calculated from neutrophils adherent to the mock (blue) or RSV (green) infected AECs after 1 hour. Thin dashed lines show median distance to nearest neighbouring neutrophil. Thick dashed lines show median distance to nearest neighbouring neutrophil assuming a uniform distribution of adherent neutrophil counts. Median distances were compared using a Wilcoxon-Mann- Whitney U test. C) Average nearest neighbour distance of neutrophils over time during migration through RSV infected AECs, calculated as above from fast time-lapse video microscopy (n=200). Mean shown with dark green line. Range (min-max) indicated in colour block. Track metrics calculated using motilityLab. Neutrophil swarming dynamics during RSV infection in a human model. (D) Time-course of migration tracks on apical side of AEC following addition of neutrophils on basolateral side. Maximal intensity projection of the first 20- (left panel) or 10-minute (middle and right panels) time intervals. Scale bars, 100 µm. (E) Time-course of neutrophil accumulation (by MFI) on the apical surface of RSV infected AECs. (F) Time course of neutrophil accumulation by number of neutrophils on apical side per time-interval is shown. (G) images and MFI (H) of a single neutrophil (#1) becoming calcein red orange-negative at 15 min and its correlation to neutrophil-amplified chemotaxis (red tracks) Scale bars, 50 µm. Neutrophil positions were processed using ImageJ (imagej.nih.gov/ij/) and coordinates analysed using R version 4.0.3. (29)

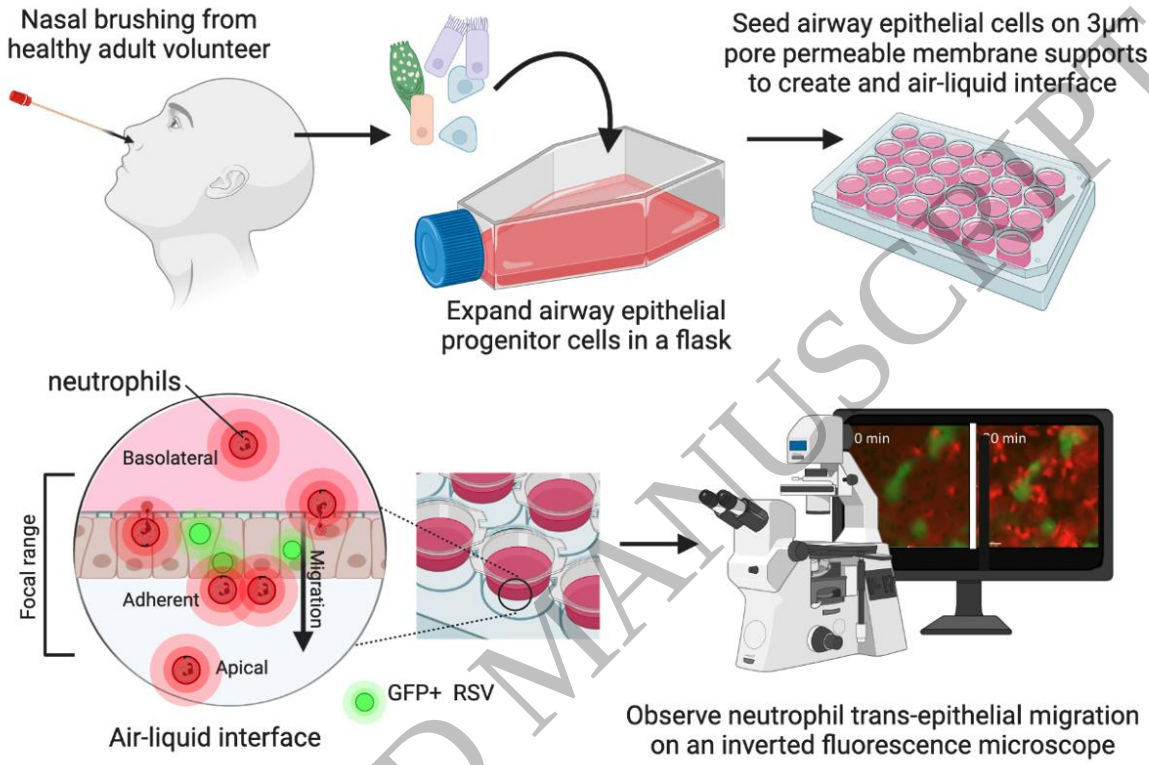

Figure 1
159x106 mm (x DPI)

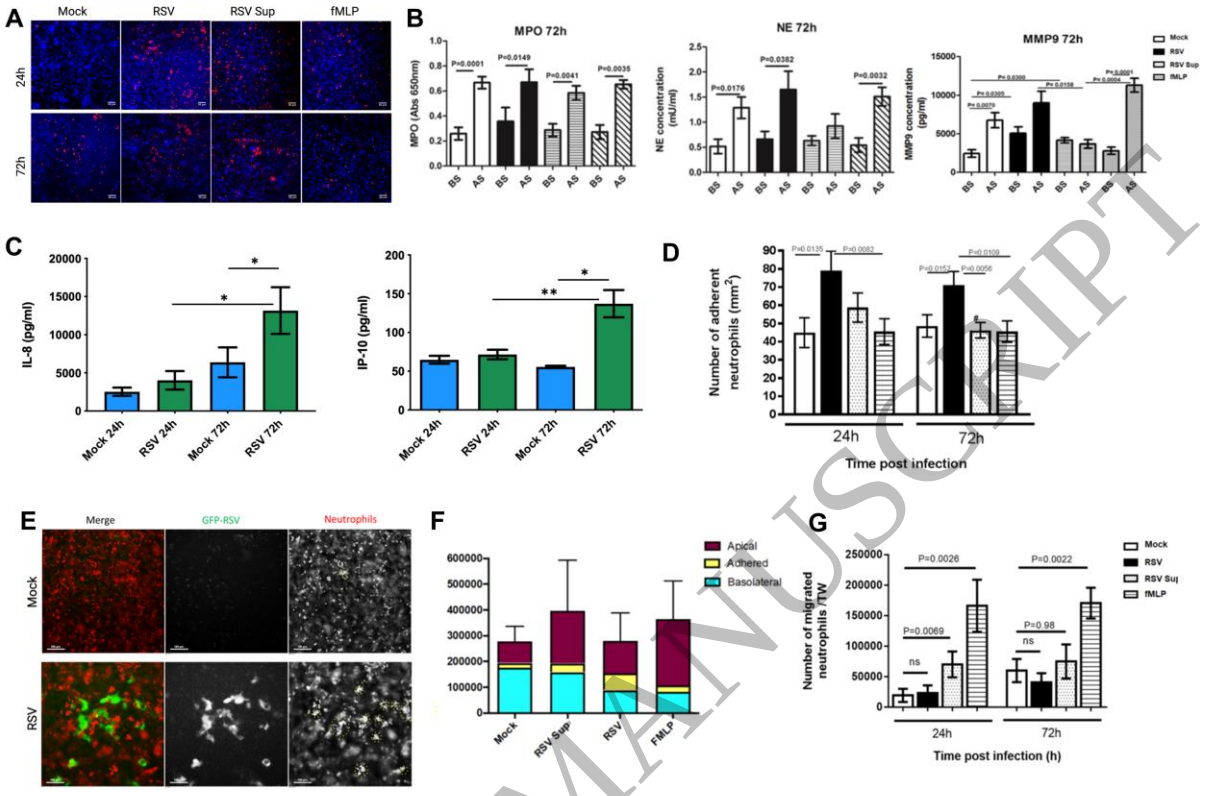

Figure 2
159x119 mm (x DPI)

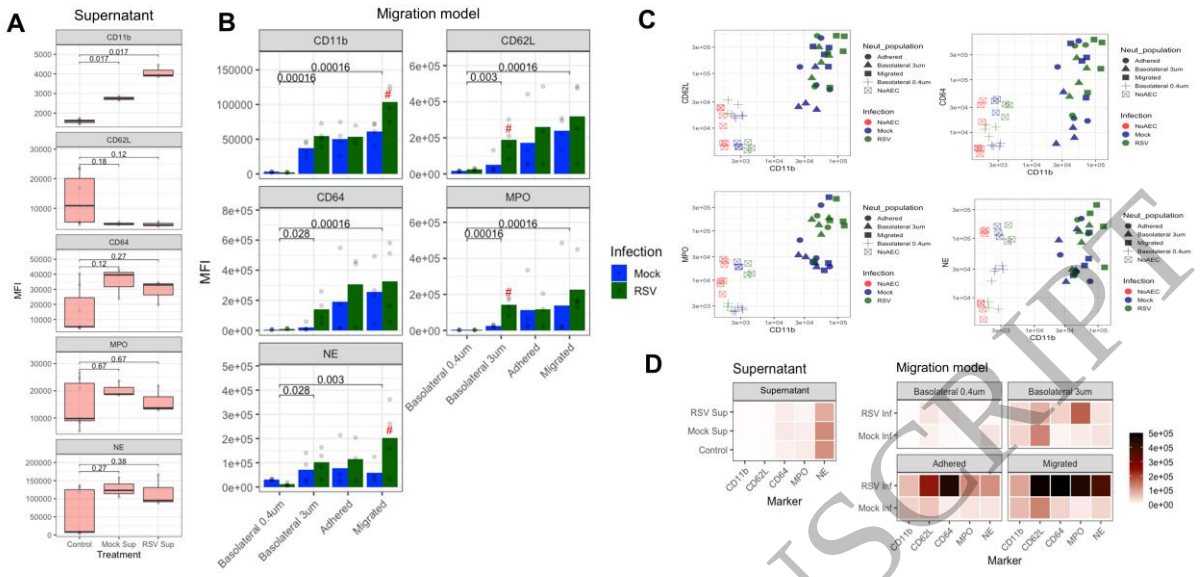

Figure 3A
159x75 mm (x DPI)

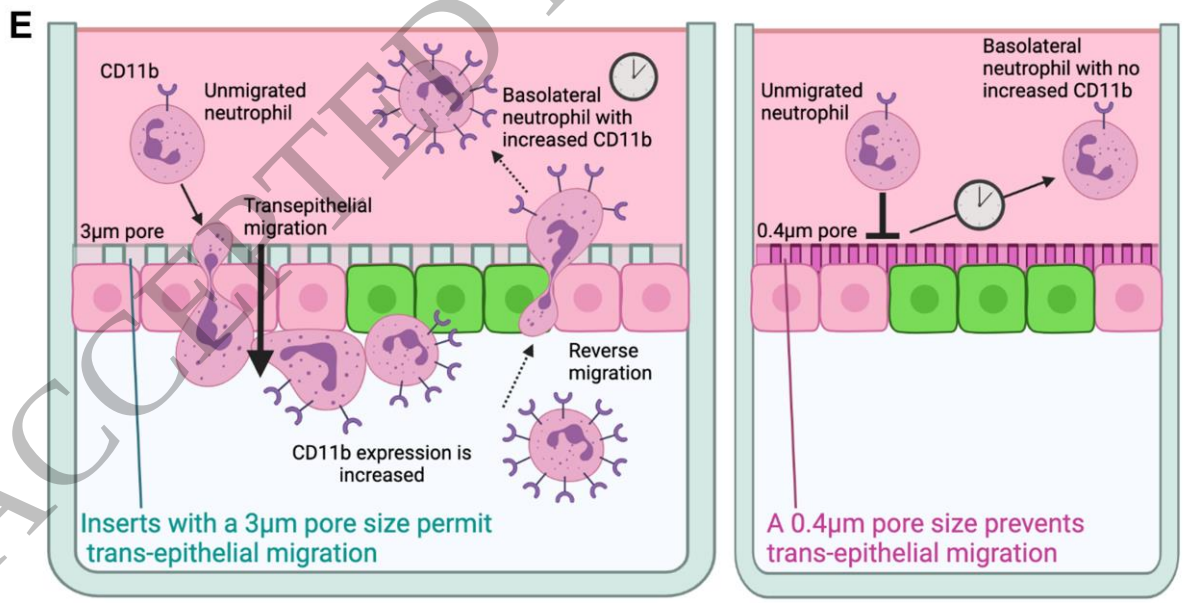

Figure 3B
159x79 mm (x DPI)

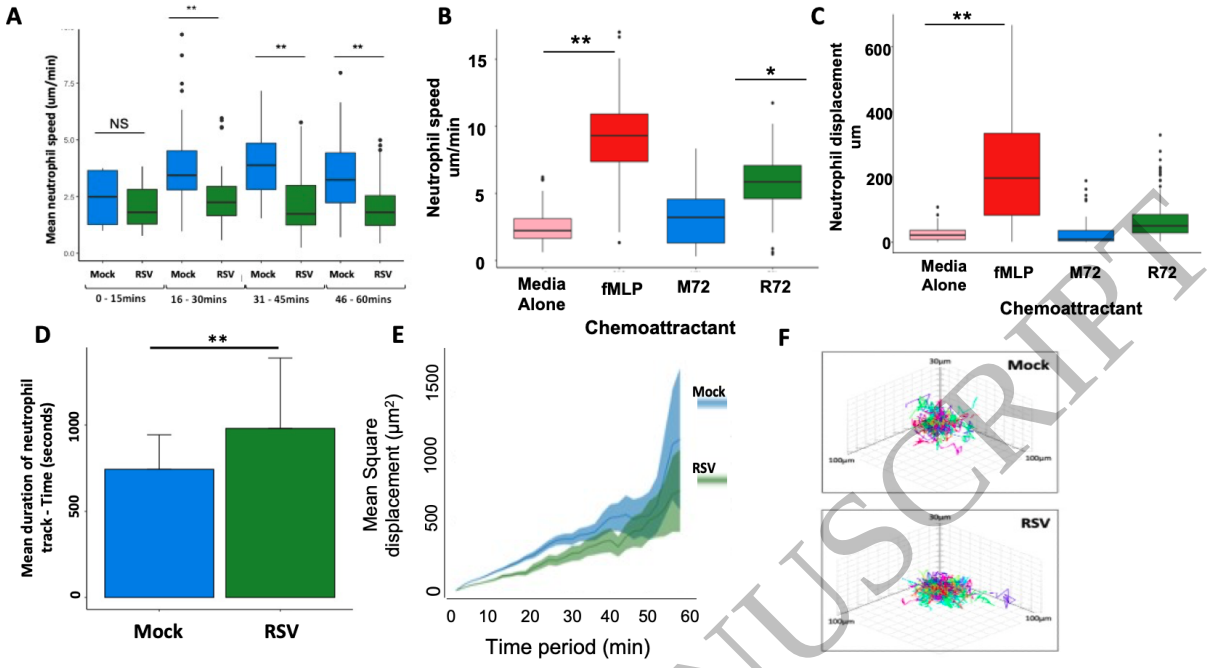

Figure 4
159x87 mm (x DPI)

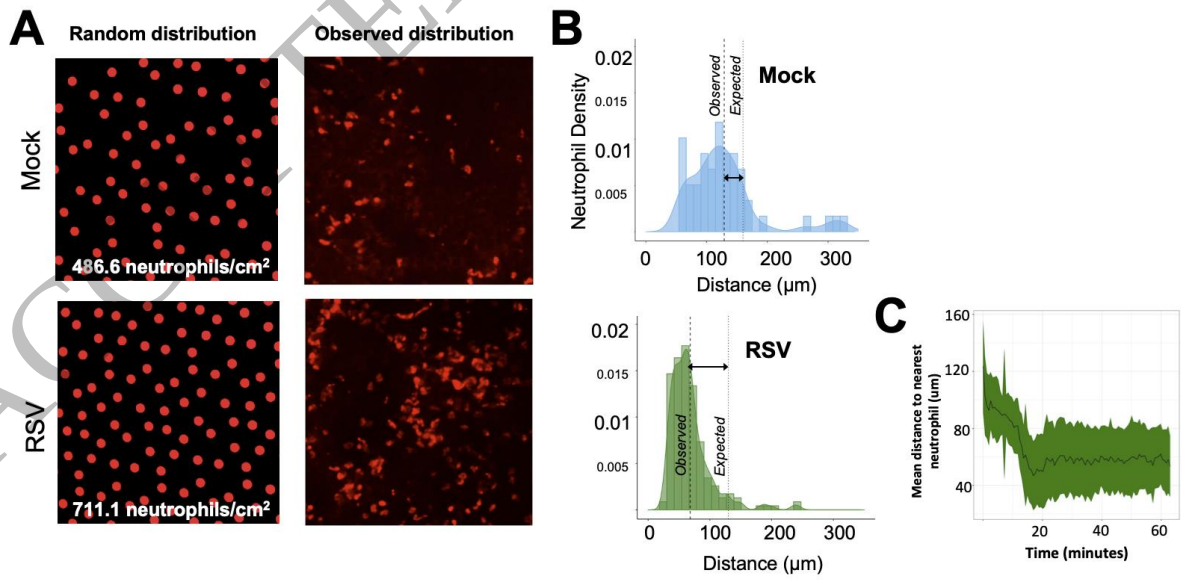

Figure 5A
159x78 mm (x DPI)

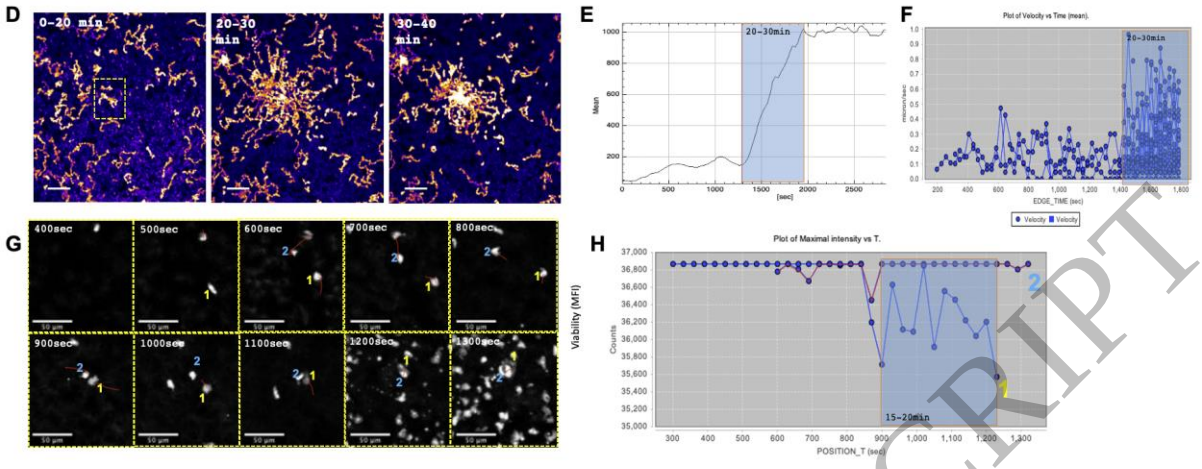

Figure 5B
159x62 mm (x DPI)